

Disentangling thermal and nonthermal excited states in a charge-transfer insulator by time- and frequency-resolved pump-probe spectroscopy

Claudio Giannetti,¹ Goran Zgrablic,² Cristina Consani,^{3,*} Alberto Crepaldi,^{3,†} Damiano Nardi,^{1,4} Gabriele Ferrini,¹ G. Dhalenne,⁵ A. Revcolevschi,⁵ and Fulvio Parmigiani^{2,3}

¹*Department of Physics, Università Cattolica del Sacro Cuore, Brescia I-25121, Italy*

²*Sincrotrone Trieste SCpA, Basovizza I-34012, Italy*

³*Department of Physics, Università degli Studi di Trieste, Trieste I-34127, Italy*

⁴*Department of Physics, Università degli Studi di Milano, Milano I-20122, Italy*

⁵*Laboratoire de Physico-Chimie de l'Etat Solide, ICMMO, CNRS, UMR 8182, Université Paris-Sud, Bat. 414, 91405 Orsay, France*

(Received 3 August 2009; published 23 December 2009)

Time- and frequency-resolved pump-probe optical spectroscopy is used to investigate the effects of the impulsive injection of delocalized excitations through a charge-transfer process in insulating CuGeO_3 . A large broadening of the charge-transfer edge is observed on the sub-ps time scale. The modification of this spectral feature cannot be attributed to the local increase in the effective temperature, as a consequence of the energy absorbed by the pump pulse. The measured modifications of the optical properties of the system are consistent with the creation of a nonthermal state, metastable on the picosecond time scale, after the pump-induced impulsive modification of the electron interactions.

DOI: [10.1103/PhysRevB.80.235129](https://doi.org/10.1103/PhysRevB.80.235129)

PACS number(s): 74.40.+k, 74.72.Hs, 78.47.J-

I. INTRODUCTION

In the last years, the investigation of the dynamics of strongly correlated systems (SCS) far from equilibrium emerged as an important but difficult and intriguing problem.¹ The fundamental questions are related to the possibility of impulsively modifying and, possibly, controlling the many-body electronic local interactions.

However, to approach this problem some fundamental questions must be considered. For example, how is described the dynamics of the electronic band structure, as the hamiltonian is modified under nonequilibrium conditions? Does the system relax to a quasithermal state corresponding to an increase in the effective local temperature after energy absorption or is the interaction so deeply modified that new nonthermal states can emerge?

Ongoing theoretical works, aimed at investigating the problem of nonequilibrium physics in quantum and correlated systems, are based on real-time diagrammatic Monte Carlo,² adaptive time-dependent density-matrix renormalization group,³ and nonequilibrium dynamical mean-field theory (DMFT) (Refs. 4 and 5) techniques. In particular, the application of DMFT to the Falicov-Kimball model⁵ evidenced that, after an impulsive variation in the local electronic interaction (interaction quench), the system relaxes to a nonthermal steady state, i.e., a state not corresponding to the increase in temperature δT related to the increase in energy absorbed by the system. The creation of a nonthermal state is possible even in the case of an infinitesimal interaction quench, i.e., when the impulsive change in the local interaction is smaller than the critical interaction U_c (U_c is the energy necessary for the occurrence of an insulator-metal transition).⁵

Optical time-resolved pump-probe experiments are a unique tool to investigate this physics, being able to directly follow the sub-ps relaxation dynamics of a system, after excitation with a femtosecond pump pulse. Different configurations, such as time-resolved optical and photoemission

spectroscopies have been recently employed to investigate the dynamics of photoinduced Mott insulator-metal transitions.^{6–11} However, to investigate the nonequilibrium dynamics of a system, in the limit of small interaction quenches, it is mandatory to develop an experimental technique capable to detect small variations in the electronic properties in a wide frequency spectral range and time domain, and to elaborate new interpretative models.

Here we report on a time-resolved optical spectroscopy with simultaneous high time and frequency resolution applied to study the nonequilibrium electronic structure of CuGeO_3 when a charge-transfer process is photoinduced by a suitable light pulse in the femtosecond time domain. The nonequilibrium optical response is investigated by ultrashort white light pulses, in a spectral range extending from 400 to 800 nm.

CuGeO_3 is characterized by the “robustness” of the insulating phase, i.e., the absence of transitions to metallic states at high temperatures, and by 1D noninteracting chains of edge-sharing Cu-O_4 plaquettes. The fine frequency resolution is exploited to observe in real time the nonequilibrium dielectric function and to follow the line profile variation in the spectral features, disentangling the thermal and nonthermal effects. In particular, we show that the photoinjection of delocalized excitations within the Cu-O_4 plaquettes, obtained by the impulsive excitation of the charge-transfer transition from the $\text{Cu } 3d$ localized states into the delocalized bands, strongly perturbs the $\text{Cu } 3d\text{-O } 2p$ transfer integral, modifying the hamiltonian and leaving the system in an excited state which is not compatible with the thermal state expected as a consequence of the local increase in temperature generated by the energy delivered by the pump pulse.

II. THERMAL VS NONTHERMAL EXCITED STATES IN A CHARGE-TRANSFER INSULATING CUPRATE

Copper-oxide-based compounds (cuprates) are one of the most important SCS family, because of the high- T_C super-

conducting phase shown by some doped systems. In general, copper oxides exhibit a variety of copper coordinations ranging from square planar to octahedral and distorted octahedral. In these compounds the Cu $3d$ orbitals contain an odd number of electrons and a metallic ground state should be expected. In contrast with the predictions of the one-electron band theory, the Coulomb energy related to the on-site repulsive electron-electron interactions overwhelms the energy width of the conduction band related to the translational symmetry, accounting for the insulating ground state.^{12,13} Cluster models have been developed to calculate, for a simple Cu_xO_y cluster,¹² the eigenvalues of the hamiltonian $H = \sum_l E_d(l) d_l^\dagger d_l + \sum_l E_p(l) p_l^\dagger p_l + \sum_l T_{pd}(l) (d_l^\dagger p_l + p_l^\dagger d_l) + H_U$, d and p being operators creating a hole in the Cu $3d$ and O $2p$ orbitals, indexed by the spin and orbital quantum number l and T_{pd} the Cu $3d$ -O $2p$ transfer integral. Electron correlations are mimicked through the interaction hamiltonian $H_U = \sum_{m,n,m',n'} U(n,n',m,m') d_m^\dagger d_{m'}^\dagger d_n^\dagger d_{n'}$, U being the repulsive local interaction and m, n, m', n' the quantum number labels. The large value of the U term is responsible for the insulating gap of the undoped cuprates. Cluster calculations qualitatively account for the charge-transfer nature of the insulating gap in undoped cuprates.

When a charge-transfer insulator, at fixed temperature T , absorbs a short and intense laser pulse, the nature of the excited state can follow two different paths. (i) Quasithermal excited state. In this case, the system is left in a thermal state described by an effective temperature $T + \delta T$, where the temperature increase corresponds to the increase in the internal energy of the system delivered by the pump pulse. The action of the pump pulse merely corresponds to a variation in the electronic distribution. In this case the relaxation dynamics can be efficiently described by the two-temperatures model.¹⁴ (ii) Nonthermal excited state. In this scenario, the excitation perturbs the T_{pd} and U terms of the hamiltonian to an extent that the ground state impulsively changes and the dynamics of the physical properties is characterized by the relaxation toward the new ground state. This new state does not correspond to a quasithermal state labeled by an effective temperature $T + \delta T$.

The most striking evidence of nonthermal states is the possibility to photoinduce insulator-metal phase transitions in a Mott insulator.⁹ However, less efforts have been devoted to investigate the dynamics of charge-transfer insulating cuprates, which do not exhibit any metal phase even when T_{pd} and U are strongly modified by the femtosecond pump pulses. In this case, the collapse of the insulating gap during the nonthermal insulator-to-metal phase transition is replaced by a weaker variation in the electronic properties of the insulating phase. For this reason it is mandatory to develop an experimental setup with high time and frequency resolution able to follow the variation in the spectral features typical of a charge-transfer insulator on the sub-ps time scale.

III. EXPERIMENT

The time and frequency resolution is obtained by focusing 60 fs-790 nm light pulses on a CaF_2 platelet to produce supercontinuum white light (SWL) at 1 kHz repetition rate.

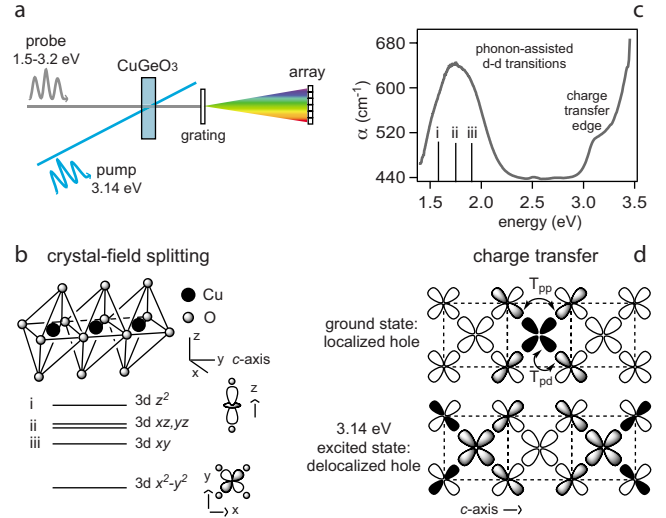


FIG. 1. (Color online) (a) Schematics of the blue pump-SWL probe experiment. (b) The sketch of the edge sharing Cu-O₆ octahedra is reported. Splitting of the level induced by the local crystal field is shown. (c) Absorption coefficient in the visible spectrum with light polarization along the c axis, taken from Ref. 15. (d) Charge distribution within the Cu-O₄ plaquettes in the ground state and delocalized excited state, as calculated through cluster models on Cu_3O_8 clusters. High, medium, and low hole densities are indicated by the black, gray, and white colors.

The SWL is focused on the sample in spatial and temporal coincidences with the 400 or 800 nm pump pulse and dispersed on a 512 pixel NMOS array, after the interaction [see Fig. 1(a)]. A complete scan of the variation in the transmissivity T is triggered by the pump pulse and completed before the following laser pulse. At the beginning, both the pump and probe polarizations are directed along the c axis [see Fig. 1(b)]. The relative variation in the transmissivity T is directly related to the pump-induced change in the absorption coefficient α through $\delta T(t)/T = -L\delta\alpha(t)$, the sample thickness being $L = 20 \mu\text{m}$. The temporal profile of SWL is characterized by means of optical Kerr effect in water. CuGeO_3 single crystals were grown from the melt by a floating zone technique.¹⁶

IV. CuGeO_3 CRYSTAL STRUCTURE AND ELECTRONIC PROPERTIES

The relevant unit of the system is a planar Cu-O₄ plaquette. In particular, while in high-temperature superconductors the Cu-O₄ units share their corners, in CuGeO_3 the Cu plaquettes are edge sharing, coordinated along the c axis [see Fig. 1(b)], and the Cu $3d$ and O $2p$ orbitals form a $\sim 98^\circ$ angle. At room temperature CuGeO_3 belongs to the orthorhombic group D_{2h} . The unit cell contains two edge sharing strongly deformed Cu-O₆ octahedra, with distances $\text{Cu-O}_{\text{apex}} = 2.77 \text{ \AA}$ and $\text{Cu-O}_{\text{inplane}} = 1.94 \text{ \AA}$.¹⁷

Because of its peculiar crystal and electronic structure, CuGeO_3 is a quite suitable simple system to study the relaxation dynamics of a charge-transfer insulating cuprate upon the impulsive injection of excitations. Figure 1(c) reports the

peculiar features of the optical absorption spectrum, when the incident light is polarized along the c axis. The absorption band at 1.5–2.1 eV is related to phonon-assisted transitions between Cu 3d levels split as a consequence of the crystal field acting on the Cu atoms.^{15,18} In particular, three oscillators can be identified at photon energies of ~ 1.6 , 1.75, and 1.9 eV, attributed to transitions from the $3d_{x^2-y^2}$ hole ground state to $3d_{xy}$, $3d_{xz,yz}$, and $3d_{z^2}$ levels¹⁹ [see Fig. 1(b)]. At photon energies larger than ~ 3 eV, the edge in the absorption coefficient [see Fig. 1(c)] is attributed to the charge-transfer process from the ground state (hole in the Cu atom) to an excited state (hole in the O atoms).¹⁸ Considering the hybridization of the O 2p orbitals with both the Cu 3d and the nearest-neighbor O 2p orbitals, the effective charge-transfer gap for the x^2-y^2 symmetry state is $\sqrt{(\Delta_{pd}-T_{pp})^2+4T_{pd}^2}$, Δ_{pd} being the energy of an hole in the O 2p orbital, T_{pd} the transfer integral between O 2p and Cu 3d orbitals and T_{pp} the overlap integral between O 2p-O 2p orbitals, including both σ and π bondings. Note that $T_{pp} \neq 0$ (and hopping of the hole to adjacent plaquettes is possible) only if the Cu-O-Cu bonding angle is different from 90° . The shoulder in the absorption coefficient at 3.1–3.2 eV [see Fig. 1(c)] is attributed to a superposition of plasmons related to transitions from the ground state, where 72% of the hole density is localized on the Cu atoms, into a delocalized final state with a high occupation probability of the neighbor plaquettes,^{13,15} as shown in Fig. 1(d). The final state corresponds to the formation of a spin-singlet state on the neighboring plaquette, known as Zhang-Rice singlet.²⁰ As a consequence of dipole selection rules, this excitonic transition can be induced only when the polarization of the light is parallel to the c axis. If the polarization is perpendicular to the c axis (along the b axis), only the charge-transfer edge survives, corresponding to injection of localized holes in the O 2p orbitals, whereas the excitonic shoulder does not contribute.

The shape of the charge-transfer edge [see Fig. 1(c)], in both c and b axis polarizations, follows the Urbach's rule:²¹

$$\alpha = \alpha_0 e^{\left[\frac{\sigma(E-E_0)}{kT}\right]}. \quad (1)$$

α_0 and E_0 being temperature-independent parameters and σ the temperature-dependent slope of $kT \ln(\alpha/\alpha_0)$, given by $\sigma = \sigma_0(2kT/E_p) \tanh(E_p/2kT)$, where E_p is the characteristic phonon energy and k the Boltzmann constant. Best-fit values for E_0 were determined to be 3.46 and 3.67 eV for light polarization parallel to the c and b axes, respectively.¹⁸ The Urbach shape of the absorption edge is a universal property of excitonic absorption edges related to exciton scattering by optical phonons.^{22,23} The values $E_p=53$ and 56 meV extracted from the fit of expression (1) to the CuGeO₃ absorption coefficients with light polarization along the c axis and b axis, respectively, match with the energy of a B_{2g} bond-bending mode of oxygen atoms at 427 cm^{-1} (see Ref. 24), confirming the dependence of the electronic charge-transfer process on the position of the oxygen atoms within the unit cell.

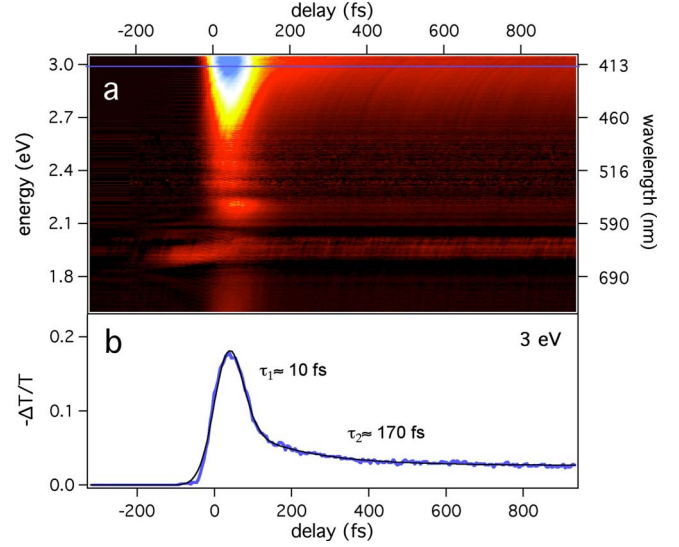


FIG. 2. (Color online) (a) Time- and frequency-transmissivity relative variation in CuGeO₃ for 3.1 eV excitation energy. Both the pump and probe beams are polarized along the c axis. The absorbed pump fluence is $\Phi_{pump}=20 \text{ mJ/cm}^2$. (b) Time trace at fixed photon energy (3 eV). The solid line is the fit to the data using a double exponential decay convoluted with a Gaussian curve.

V. RESULTS

Impulsive injection of delocalized excitations is obtained by optical pumping with coherent light pulses at 3.14 eV and polarized along the c axis. In Fig. 2(a) the relative transmissivity variation $\Delta T/\mathcal{T}(\omega, t)$ in CuGeO₃, upon excitation by 20 mJ/cm^2 pump fluence, is reported for time delays between ~ -300 and ~ 900 fs and in the spectral range between $\sim 770 \text{ nm}$ (1.6 eV) and $\sim 410 \text{ nm}$ (3 eV), covered by the supercontinuum probe pulse. The two-dimensional trace directly contains information on the variation in the imaginary part of the dielectric function during the photoexcitation of the delocalized holes in the system. The insulating charge-transfer gap appears to be impulsively quenched, resulting in a $\Delta T/\mathcal{T}(\omega)$ variation decreasing from the blue to the near-IR region (1.6 eV). $\Delta T/\mathcal{T}(\omega, t)$ scales linearly, as the pump fluence is increased, up to an energy where permanent damages are induced in the sample. In Fig. 2(b) we report the time trace of $\Delta T/\mathcal{T}(\omega)$ at 3 eV photon energy, evidencing the dynamics of the transmissivity variation. Three different time scales are observed. A fast one ($\tau_1 \sim 10$ fs), smaller than the pulse duration,²⁵ a slower one ($\tau_2 \sim 170$ fs) responsible for the relaxation on the sub-ps time scale and a very slow one that extends to several hundreds of picosecond. While the value of τ_1 assesses the electronic nature of this fast process, the slower dynamics, revealed by τ_2 , contains the information on the energy-relaxation process (cooling), through the electron-phonon coupling, for both the photoinjected holes in the O 2p orbitals and the electrons in the Cu 3d correlated bands, eventually leading to the formation of a new metastable electronic and/or structural phase. The two fast dynamics are evident reporting the time-resolved spectra of $\Delta T/\mathcal{T}(\omega, t)$ at different delay times [see Fig. 3(a)]. The transmissivity is impulsively quenched within the pulse duration

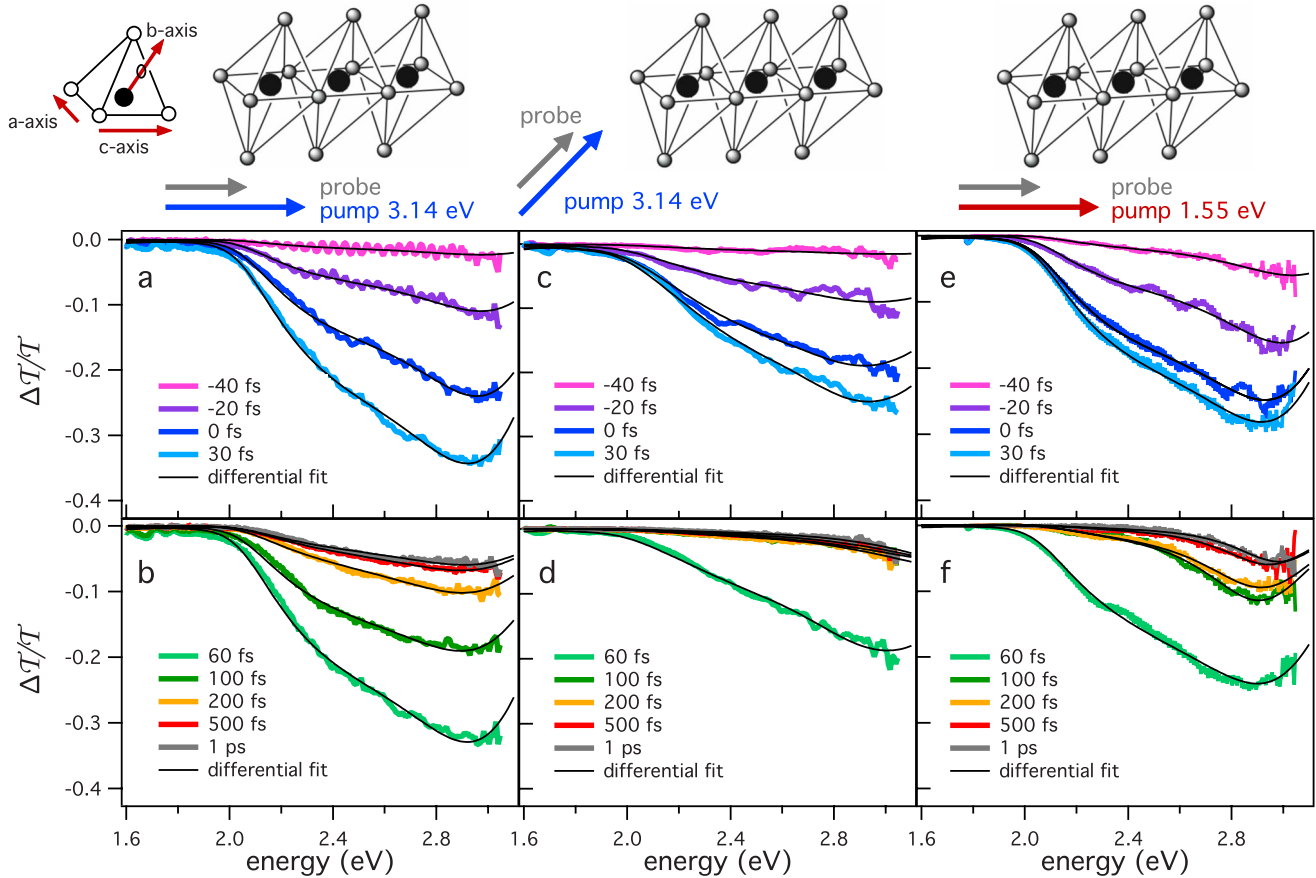


FIG. 3. (Color online) Slices of the two-dimensional $\Delta T/T(\omega, t)$ spectrum at different delay times and different pump polarizations and wavelengths. The solid lines are the fit to the data of the differential dielectric function.

(~ 60 fs), monotonically decreasing moving from the near-IR (~ 1.6 eV) to the blue (~ 3 eV), with a plateau around 3 eV and a kink at about 2.3 eV. After the excitation with the pump pulse, $\Delta T/T(\omega, t)$ relaxes toward the equilibrium, maintaining, for several hundreds of ps, a broad transmissivity variation in the 2–3 eV range [see the spectrum at 1 ps in Fig. 3(b)].

The physics emerging from these observations is summarized in the following. The pump pulses at 3.14 eV impulsively inject a high density of excitations in the Cu-O_4 plaquettes. The absorbed fluence can be reported in terms of the ratio between the absorbed density of photons n_{ph} and the density of copper ions $n_{\text{Cu}} \approx 17 \times 10^{21} \text{ cm}^{-3}$. In particular, we obtain $n_{ph}/n_{\text{Cu}} \approx \Phi_{pump} \alpha / n_{\text{Cu}} \approx 0.1-0.2\%$, being $\alpha = 500 \text{ cm}^{-1}$. Considering the rapid delocalization of each hole within about five neighboring plaquettes,¹³ it is possible to conclude that, during the pulse duration, $\sim 0.5-1\%$ of the Cu-O_6 units are driven to the excited state where the correlated $3d$ bands are locally filled by an electron and a hole is shared among the O $2p$ orbitals and the Cu $3d$ levels of the neighboring plaquettes [see Fig. 1(d)], possibly altering both the interaction U and the transfer integral T_{pd} , and leaving the system in a metastable nonthermal phase. On the picosecond time scale, the nonequilibrium holes in the plaquettes relax following two possible pathways: (i) they can directly couple to the lattice, increasing its effective temperature; (ii) they can readily interact with the Cu $3d$ equilibrium holes,

creating a nonequilibrium population within the Cu $3d$ bands. To disentangle these effects and to clarify the role of the delocalized excitons we repeated the $\Delta T/T(\omega, t)$ measurements, maintaining constant the absorbed pump fluence, at: (i) 3.14 eV pump photon energy with polarization along the b axis. In this case, the excitonic delocalized transitions are strongly quenched and the relaxation dynamics of localized holes in the O $2p$ orbitals can be accessed; (ii) 1.55 eV pump photon energy with polarization along the c axis. Under these conditions, the pump energy is exclusively absorbed by phonon-assisted Cu $3d-3d$ intraband transitions and the dynamics is expected to be dominated by the cooling of the nonequilibrium distribution of excitations, within the Cu $3d$ bands, through electron-phonon scattering.

In Figs. 3(c) and 3(d) we report the fast and slow dynamics of $\Delta T/T(\omega, t)$ with both the pump and probe polarizations parallel to the b axis. In this case, the formation of delocalized excitons within the Cu-O_4 plaquette chains is quenched by the dipole selection rules. The fast dynamics is similar to the previous case, whereas the $\Delta T/T(\omega, t)$ variation on the picosecond time scale is drastically quenched and, ~ 100 fs after the pump pulse, the spectrum in the 2.8–3 eV energy range shows minor variations. After about 1 ps, the time-resolved spectra do not change their shape considerably, remaining constant for several hundreds of picosecond.

In Figs. 3(e) and 3(f) we report the fast and slow dynamics of $\Delta T/T(\omega, t)$ by pumping the system using pulses at 1.55

eV linearly polarized along the c axis of the crystal. The main differences from the previous cases are detected for spectra taken for $100 \text{ fs} < t < 1 \text{ ps}$ [Fig. 3(f)], where $\Delta T/T(\omega, t)$ exhibits a maximum around 2.9 eV and a kink at about 2.3 eV. After about 1 ps from the pump excitation, a large variation in the transmissivity, mostly in the 2.6–3 eV energy region, is measured, remaining constant for several hundreds of picosecond.

VI. DISCUSSION

To perform a quantitative study of the $\Delta T/T(\omega, t)$ measurements, a differential dielectric function model has been fitted to the data, i.e., the variation in $\epsilon(\omega)$ has been calculated as $\delta\epsilon(\omega) = \epsilon_L(\omega) - \epsilon_0(\omega)$, $\epsilon_0(\omega)$ being the dielectric function of CuGeO_3 in the ground state.²⁶ Notably, the best fit to the data has been obtained by employing, for all the time delays and all the pump polarizations and wavelengths, a single Lorentz oscillator $\epsilon_L(\omega) = \omega_p^2 / (\omega_0^2 - \omega^2 - i\gamma\omega)$, ω_p and ω_0 being the plasma and resonance frequencies, and γ the linewidth. In Fig. 3 the best differential fits are superimposed to the data. The main features of the measured $\Delta T/T(\omega, t)$ are reproduced by a Lorentz oscillator centered in the blue region of the spectrum. This result suggests that the physics behind the measured variation in the spectrally resolved transmissivity is essentially related to the variation in the charge-transfer edge.

Figure 4(a) reports the imaginary part of $\epsilon_L(\omega)$ during the relaxation process when the 3.14 eV pump is polarized along the c axis. The resonance frequency, starting from the equilibrium value $\hbar\omega_0 = 3.46 \text{ eV}$, decreases to 2.9 eV within $\sim 100 \text{ fs}$, remaining constant up to the picosecond time scale. The shift of $\hbar\omega_0$ is responsible for the plateau around 3 eV, observed in the $\Delta T/T(\omega, t)$ spectra [see Figs. 3(a) and 3(b)]. The width of the Lorentzian profile is impulsively broadened to about 2 eV within the pulse duration and recovers a constant value of 1.2 eV. This feature is responsible for the broad variation in the transmissivity in the 2–3 eV range [see Fig. 3(b)].

In Fig. 4(b) we report the imaginary part of $\epsilon_L(\omega)$ during the relaxation process, when the 3.14 eV pump is polarized along the b axis. The resonance frequency appears at the equilibrium value $\hbar\omega_0 = 3.67 \text{ eV}$ and impulsively decreases to 3.14 eV, recovering, approximately, the 3.67 eV equilibrium value on the time scale of the pump and probe pulses cross-correlation.²⁷ The width of the Lorentzian profile, impulsively broadened to about 2 eV, recovers a constant value of 0.3 eV after the excitation. The rapidity of the recovery of the $\hbar\omega_0$ and γ equilibrium values explains the relatively small shape variations in the time-resolved spectra after $\sim 200 \text{ fs}$ [see Fig. 3(d)], in comparison with the previous case.

Figure 4(c) shows the dynamics of $\text{Im } \epsilon_L(\omega)$ when the system is excited by 1.55 eV pump pulses polarized parallel to the c axis. Comparing the measured $\Delta T/T(\omega, t)$ to the results obtained at 3.14 eV pump energy and with the same polarization [see Fig. 4(a)], the $\hbar\omega_0$ shift from 3.46 to 2.9 eV is similar, whereas the broadening of the linewidth is much more limited ($\gamma \sim 0.6 \text{ eV}@1 \text{ ps}$). A clear oscillation of γ ,

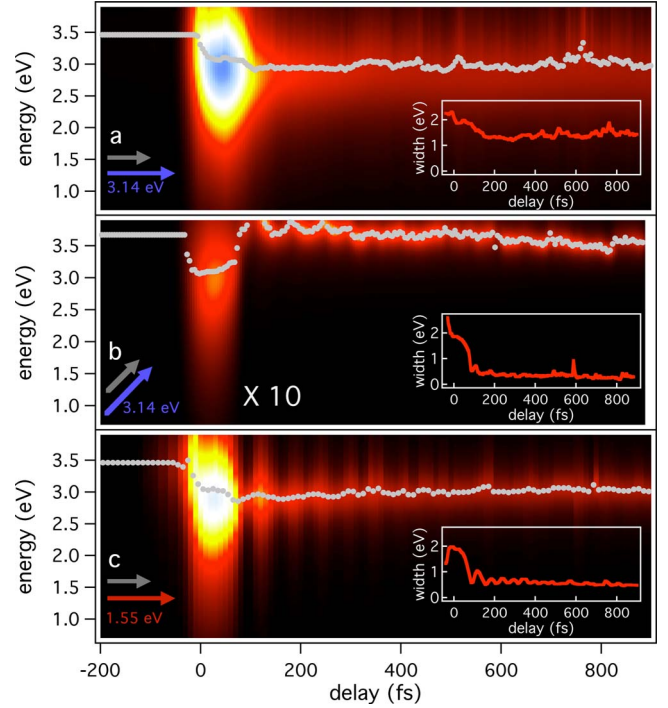


FIG. 4. (Color online) (a)–(c) Temporal dynamics of $\text{Im } \epsilon_L$ at different pump polarizations and wavelengths, as obtained from the differential fitting procedure. The color scales have been normalized to the maximum variation detected. The color scale in Fig. 4(b) has been multiplied by a factor 10. The gray dots indicate the resonance frequencies $\hbar\omega_0$. The insets display the temporal dependence of the Lorentzian linewidths γ .

with a period of $\sim 54 \text{ fs}$, is observed at 1.55 eV pump photon energy [see Fig. 4(c)]. This oscillation can be attributed to the dispersive coherent excitation²⁸ of an A_g optical mode at 594 cm^{-1} , related to the bond-stretching vibration along the c axis of apical oxygens.²⁴ This finding is rather interesting since it confirms the strong dependence of the charge-transfer process on the lattice structure.

Comparing the different set of data, the origin of the spectrally resolved transmissivity variation in CuGeO_3 , when delocalized excitons are photoinjected in the system, is clarified. A 0.6 eV shift of the resonance frequency of the charge-transfer edge is observed either when the pump photon energy is 3.14 or 1.55 eV. This result confirms that, when the charge-transfer process is excited by c -polarized pump pulses, the holes, shared among the O $2p$ orbitals and the Cu $3d$ levels of the neighboring plaquettes, strongly interact with the Cu $3d$ equilibrium holes, creating a nonequilibrium population within the Cu $3d$ bands. For this reason, the 0.6 eV shift can be attributed to the creation of a nonequilibrium distribution of excitations within the Cu $3d$ bands. In particular, the measured resonance frequency decrease is compatible with a decrease in the energy needed to move a hole from the Cu $3d$ levels to the O $2p$ orbitals ($\delta\Delta_{pd} \sim 0.6 \text{ eV}$), since the higher crystal-field split $3d$ levels [see Fig. 1(b)] are occupied, on average, by the nonequilibrium population within the Cu $3d$ bands, created by the pump pulse. On the contrary, the large broadening of the charge-transfer edge, measured when the system is excited by 3.14 eV c -polarized

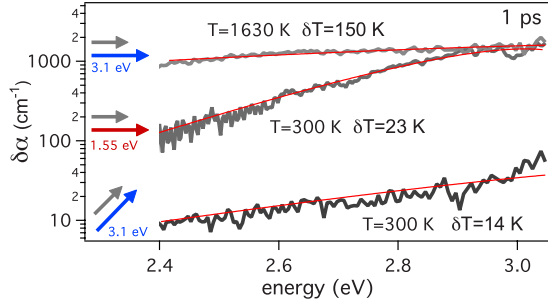


FIG. 5. (Color online) Variation in the absorption coefficient, as a function of the probe energy, at 1 ps delay time. The solid lines are the fit of expression (2) to the data, being the effective local temperature T and temperature increase δT the only free parameters.

pump pulses, has no counterpart in all other configurations. This result suggests that the observed charge-transfer broadening is a genuine effect of the delocalized excitons photo-injected in the Cu-O₄ planes mainly altering the T_{pd} term of the Hamiltonian and leaving the system in a metastable nonthermal phase.

New insights into the origin of the metastable state created by the pump excitation are given by the analysis of the time-resolved spectra at 1 ps. At this time delay, the cooling processes related to electron-phonon scattering are over and, at $t > 1$ ps, the spectra slowly decay on the sub-ns time scale. The nonthermal nature of the charge-transfer broadening, when delocalized excitons are photo-injected, can be argued recalling the Urbach's rule. Differentiating the expression (1), δT being the differential increase in the temperature,

$$\delta\alpha = \alpha_0 e^{\left[\sigma(E-E_0/kT)\right]} \left[\sigma \frac{E_0 - E}{kT^2} + \frac{\partial\sigma}{\partial T} \frac{E - E_0}{kT} \right] \delta T \quad (2)$$

and taking the logarithm of Eq. (2), neglecting the $\partial\sigma/\partial T$ term, we obtain

$$\ln(\delta\alpha) = \ln(\alpha_0 \delta T) + \ln\left(\sigma \frac{E_0 - E}{kT^2}\right) + \sigma \frac{E - E_0}{kT}, \quad (3)$$

where the linear slope of $\ln(\delta\alpha)$, typical of the Urbach's law, is corrected by a $\ln[\sigma(E_0 - E)/kT^2]$ term. In Fig. 5 we report, in log scale, the $\delta\alpha$, measured after 1 ps from the pump pulse, as a function of the probe energy. The nonlinear correction to the standard Urbach's shape is evident, particularly in the c -polarized pump configurations.

The expression (2) has been fitted to the data, T and δT being the only free parameters.²⁹ In the 1.55 eV c -polarized and 3.14 eV b -polarized configurations, the slopes of the measured $\delta\alpha$ are compatible with an effective local temperature of $T=300$ K, the temperature increase being $\delta T=23$ and 14 K, respectively. These results must be compared with the estimated lattice heating due to the absorbed pump energy. This is given by: $\delta T = I\alpha/C_{lat}$, where $I \approx 20$ mJ/cm² is the

absorbed pump fluence and $C_{lat}=2.77$ JK⁻¹ cm⁻³ the CuGeO₃ heat capacity.³⁰ Assuming $\alpha=500$ and 250 cm⁻¹ in the 1.55 eV c -polarized and 3.14 eV b -polarized configurations,¹⁵ we can estimate $\delta T=3.6$ K and 1.8 K, respectively. While the ratio of the estimated temperature increases (3.6 K/1.8 K \approx 2), related to the difference in the absorbed density of energy, is compatible with measured ratio (23 K/14 K \approx 1.6), the discrepancy of the absolute values can be attributed to the fact that the energy absorbed by the electronic transitions is delivered to a subset of optical lattice modes, i.e., strongly coupled optical phonons (SCOPs).³¹ Therefore, the charge-transfer edge broadening, sensitive to the exciton scattering by optical phonons, reflects an effective temperature of the SCOPs higher than the temperature estimated considering the heat capacity of the whole lattice modes.

In contrast to the previous cases, when the system is excited by c -polarized 3.14 eV pump pulses and delocalized excitations are photo-injected in the O 2*p* orbitals, the measured $\delta\alpha$ is fitted assuming an effective local temperature of 1630 K and a temperature increase of $\delta T=150$ K (see Fig. 5), values incompatible with a quasithermal physical scenario. These results confirm that the linewidth broadening measured in this configuration [see Figs. 3(b) and 4(a)] is of nonthermal origin, i.e., it cannot be attributed to the local heating of the lattice.

VII. CONCLUSIONS

In conclusion, we have applied a time- and frequency-resolved technique to investigate the excited-state dynamics of a model strongly correlated system as CuGeO₃. The evolution of the dielectric function on the sub-ps time scale indicates that the impulsive injection of holes delocalized on the O 2*p* oxygen orbitals strongly perturbs the potential experienced by electrons on the Cu 3*d* levels, leaving the system in a nonthermal metastable (on the picosecond time scale) phase. The possibility to follow the decay dynamics of the electronic properties of a charge-transfer insulating cuprate system, impulsively driven in a nonequilibrium state, constitutes a further step toward the understanding of the puzzling physics of these systems. In addition, the experimental investigation of the nonthermal states, obtained after the impulsive variation in the potential experienced by electrons in CuGeO₃, can be regarded as a benchmark test for the development of more realistic theoretical models for the non-equilibrium physics of strongly correlated systems.

ACKNOWLEDGMENTS

We acknowledge valuable discussions from D. Vollhardt, M. Kollar, and M. Eckstein. This work was supported in part by the Italian Ministry of University and Research under Grants No. FIRB-RBAP045JF2 and No. FIRB-RBAP06AWK3.

- *Present address: École Polytechnique Fédérale de Lausanne (EPFL), Laboratoire de Spectroscopie Ultrarapide, CH-1015 Lausanne, Switzerland.
- †Present address: École Polytechnique Fédérale de Lausanne (EPFL), Institut de Physique des Nanostructures, CH-1015 Lausanne, Switzerland.
- ¹J. K. Freericks and V. Zlatić, *Rev. Mod. Phys.* **75**, 1333 (2003).
 - ²M. Schiró and M. Fabrizio, *Phys. Rev. B* **79**, 153302 (2009).
 - ³S. R. Manmana, S. Wessel, R. M. Noack, and A. Muramatsu, *Phys. Rev. B* **79**, 155104 (2009).
 - ⁴M. Eckstein and M. Kollar, *Phys. Rev. B* **78**, 205119 (2008).
 - ⁵M. Eckstein and M. Kollar, *Phys. Rev. Lett.* **100**, 120404 (2008).
 - ⁶T. Ogasawara, M. Ashida, N. Motoyama, H. Eisaki, S. Uchida, Y. Tokura, H. Ghosh, A. Shukla, S. Mazumdar, and M. Kuwata-Gonokami, *Phys. Rev. Lett.* **85**, 2204 (2000).
 - ⁷S. Iwai, M. Ono, A. Maeda, H. Matsuzaki, H. Kishida, H. Okamoto, and Y. Tokura, *Phys. Rev. Lett.* **91**, 057401 (2003).
 - ⁸M. Chollet, L. Guerin, N. Uchida, S. Fukaya, H. Shimoda, T. Ishikawa, K. Matsuda, T. Hasegawa, A. Ota, H. Yamochi, Gunzi Saito, Ryoko Tazaki, Shin-ichi Adachi, and Shin-ya Koshihara, *Science* **307**, 86 (2005).
 - ⁹L. Perfetti, P. A. Loukakos, M. Lisowski, U. Bovensiepen, H. Berger, S. Biermann, P. S. Cornaglia, A. Georges, and M. Wolf, *Phys. Rev. Lett.* **97**, 067402 (2006).
 - ¹⁰H. Okamoto, H. Matsuzaki, T. Wakabayashi, Y. Takahashi, and T. Hasegawa, *Phys. Rev. Lett.* **98**, 037401 (2007).
 - ¹¹C. Kübler, H. Ehrke, R. Huber, R. Lopez, A. Halabica, R. F. Haglund, Jr., and A. Leitner, *Phys. Rev. Lett.* **99**, 116401 (2007).
 - ¹²H. Eskes, L. H. Tjeng, and G. A. Sawatzky, *Phys. Rev. B* **41**, 288 (1990).
 - ¹³S. Atzkern, M. Knupfer, M. S. Golden, J. Fink, A. Hübsch, C. Waidacher, K. W. Becker, W. von der Linden, M. Weiden, and C. Geibel, *Phys. Rev. B* **64**, 075112 (2001).
 - ¹⁴S. Anisimov, B. Kapeliovich, and T. Perel'man, *Sov. Phys. JETP* **39**, 375 (1974).
 - ¹⁵S. Pagliara, F. Parmigiani, P. Galinetto, A. Revcolevschi, and G. Samoggia, *Phys. Rev. B* **66**, 024518 (2002).
 - ¹⁶A. Revcolevschi and G. Dhalenne, *Adv. Mater. (Weinheim, Ger.)* **5**, 657 (1993).
 - ¹⁷H. Völlenkle, A. Wittmann, and H. Nowotny, *Monatsch. Chem.* **98**, 1352 (1967).
 - ¹⁸M. Bassi, P. Camagni, R. Rolli, G. Samoggia, F. Parmigiani, G. Dhalenne, and A. Revcolevschi, *Phys. Rev. B* **54**, R11030 (1996).
 - ¹⁹C. de Graaf and R. Broer, *Phys. Rev. B* **62**, 702 (2000).
 - ²⁰F. C. Zhang and T. M. Rice, *Phys. Rev. B* **37**, 3759 (1988).
 - ²¹F. Urbach, *Phys. Rev.* **92**, 1324 (1953).
 - ²²S. Schmitt-Rink, H. Haug, and E. Mohler, *Phys. Rev. B* **24**, 6043 (1981).
 - ²³J. Dow and D. Redfield, *Phys. Rev. B* **5**, 594 (1972).
 - ²⁴Z. V. Popović, S. D. Dević, V. N. Popov, G. Dhalenne, and A. Revcolevschi, *Phys. Rev. B* **52**, 4185 (1995).
 - ²⁵The value $\tau=10$ fs has been extracted by fitting the convolution of the pump and probe pulses with a double exponential decay function to the experimental data.
 - ²⁶The dielectric function of CuGeO₃ in the ground state has been obtained by fitting, for both *b* and *c* polarizations, the absorption coefficient reported in Ref. 15 with a multioscillator model.
 - ²⁷Due to the small variations in the time-resolved spectra, the value of $\hbar\omega_0=3.67$ eV, determined through the differential fitting procedure, is subjected, on the sub-ps timescale, to an error larger than in the other configurations.
 - ²⁸H. J. Zeiger, J. Vidal, T. K. Cheng, E. P. Ippen, G. Dresselhaus, and M. S. Dresselhaus, *Phys. Rev. B* **45**, 768 (1992).
 - ²⁹The values of α_0 , E_0 , and σ , for both *c* and *b* polarizations, have been taken from Ref. 18 and kept fixed during the fitting procedure.
 - ³⁰M. Weiden, J. Köhler, G. Sparr, M. Köppen, M. Lang, C. Geibel, and F. Steglich, *Z. Phys. B: Condens. Matter* **98**, 167 (1995).
 - ³¹T. Kampfrath, L. Perfetti, F. Schapper, C. Frischkorn, and M. Wolf, *Phys. Rev. Lett.* **95**, 187403 (2005).